Research Journal of Applied Sciences, Engineering and Technology 6(6): 950-960, 2013
ISSN: 2040-7459; e-ISSN: 2040-7467

Submitted: October 06, 2012 Accepted: December 03, 2012 Published: June 30, 2013

Finite Element Model for the Behavior of Partially Restrained High Strength Web Angle Connections

[1]S. Taufik and [2]S. Baharom
[1]Department of Civil and Structural Engineering, Lambung Mangkurat University, Banjarmasin, 70123 Indonesia
[2]Department of Civil and Structural Engineering, National University of Malaysia, UKM Bangi 43600, Malaysia

Abstract: This study investigates the behavior of Partially Restrained (PR) connections with high strength steel through the use of Finite Element (FE) modeling. The connection model is such that double web angles are represented by radiused corner section shell elements. The full interaction between the angle and the beam and/or column is simulated by the contact element.The analysis of the moment- rotation relationship and behavior characteristics of the connection with high strength steel are compared and discussed. It is established that the contact elements and strength enhancements of the corner regions employed in this model are important parameters for accurate predictions of Double Web Angle (DWA) connection behavior with cold-formed high strength steel. The proposed connection FE model is capable making highly accurate predictions about the ultimate load capacity and the plastic strain pattern. The model presented provides excellent results for significantly increasing the connection capacity as a result of employing a higher strength steel section. A power model expression was proposed to predict the ultimate moment and initial stiffness of the high strength DWA connection. A reasonable prediction was obtained for high strength PR connection.

Keywords: Cold-formed, high strength steel, moment capacity, partially restrained, radiused corner, web angle

INTRODUCTION

Finite Element (FE) analysis of beam-column connection has been performed by many researchers. Three-dimensional FE models have been well verified by comparison with experimental results. More recent studies using FE modeling have focused mostly on the top-and-seat angle and end plate connections. The FE model from Bose *et al.* (1996), Bursi and Jaspart (1998), Citipitouglu *et al*. (2002) and Maggi *et al*. (2005), considers solid elements, while Bahaari and Sherbourne (1996) and Sherbourne and Bahaari (1996), have proposed a model with shell elements. Danesh *et al*. (2007), consider a top-and-seat angle without a web angle connection under the effect of shear force on the initial stiffness. Citipitouglu *et al*. (2002) has presented refined 3D finite element modeling of partially restrained connections including the effect of slip. Taufik and Xiao (2005 and 2006a), have studied the behavior of angle-bolted connections by using shell elements for high strength steel. Very little information has been established regarding the beam-column bolted connection with high strength steel, which Puthli and Fleischer (2001) and Moze and Beg (2011) have recently experimentally tested on a simple bolted connection. Taufik *et al*. (2011) haspredictedthe connection behavior of top and seat angle connections with high strength steel.

In this study, a bolted connection is modelled using a refined 3D modelling technique, recognizing contact effects and bolt geometry. However, modeling approach still needs to be simplified to reduce the computational effort. Shell elements are considered to eliminate the generation of various types of detailed 3D geometries. The shank and bolt hole model is introduced to refine the previous model as conducted by previous finite element modeling (Taufik and Xiao, 2006b; Taufik *et al*., 2011). In this study, the modelling will take into account the extent of corner strength enhancement of cold-formed angle cleats. Karren (1967) and Guoa *et al*. (2007) have performed experimental testing on cold-formed steel sections. Moze and Beg (2011) produced experimental testing data on high strength steel. Lewitt *et al.* (1996) conducted experimental testing on bolted column-beam connections, such as web angle connections. The connection model is such that the angle cleats are represented by radiused corner section shell elements. Various grades of high strength steel angle cleats are simulated to investigate the connection behavior.

Corresponding Author: S. Baharom, Department of Civil and Structural Engineering, National University of Malaysia, UKM Bangi 43600, Malaysia.

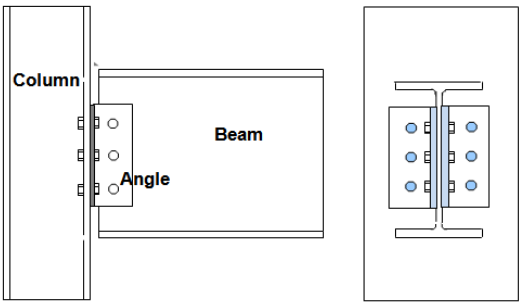

Fig. 1: Configuration details of the DWA connection

CONNECTION CONFIGURATION

Double Web Angle (DWA) connections are designated to be type of Partially Restrained (PR) connections. A DWA connection is able to transfer not only the vertical reaction but also some end moment of the beam to the column. The geometry of the DWA is based on two different sizes of beams and columns with all the connection parts remaining the same size, while the angles are clamped on beam webs. The geometry of the connection and beam depth must be adjusted to improve the connection performance. The higher strength of the cold-formed angle used, helps to maintain original connection geometry to improve the moment and rotational capacity, while the other connection components are constructed of carbon steel. The configuration details of the DWA connection in the numerical model are illustrated in Fig. 1. Both three and four rows of bolt configurations are investigated with different sized beams and angles.

FINITE ELEMENT MODEL

The ANSYS version 10.0, which is a general purpose finite element package, is selected to perform the numerical modelling analysis. A DWA connection is constructed with the beam web bolted to the column flange with a double web angle. Nonlinear DWA connection models are symmetric about the center of the beam web and no lateral displacement is assumed; consequently, only one side of the plane of symmetry is modeled. The geometry of the model thus represents one half of the full scale connection in terms of the area and moment of inertia; therefore, the capacity determined by connection model is only half of the actual load capacity. The following ANSYS element types are used for one half of the connection. Plastic shell elements (SHELL143) are used to model the beams, columns and angles. Bolt heads and nuts are modelled using eight-node isoparametric solid elements (SOLID45). The bolt heads and nuts are modelled as hexagons. The bolt shanks are modeled using twelve 3D spar elements (LINK8) connecting the farthest corner nodes of the bolts heads and nuts to each other,

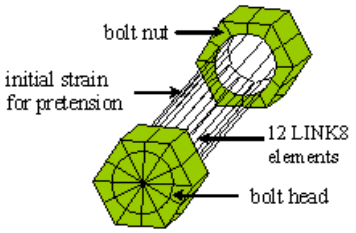

Fig. 2: Finite element models of the bolt and nut

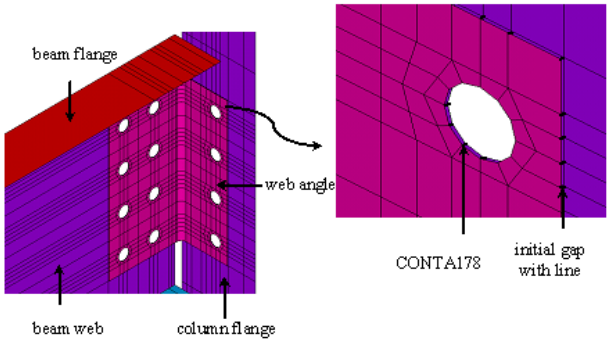

Fig. 3: Contact elements for the DWA connection

as shown in Fig. 2. The effective area of the bolt is divided into twelfths, with one twelfth per spar element. The bolt holes are modeled as circular (M22). The bolt pretension caused by bolt tightening is simulated by applying equivalent initial strains to each bolt shank element. The initial strain value of the bolt pretension is selected according to the bolt pretension calibration curves, as reported by Citipitouglu *et al*. (2002). Because the bolt is tightened, the head and/or nut stay in close contact with their connecting angles and flanges; therefore the bolts share their nodes with the plate nodes.

The interactions between the angle and the column/beam are simulated by interface elements (CONTACT178); shown in Fig. 3. The interface elements are considered to accommodate the effects of friction and slip. A friction coefficient value of 0.25 is used to capture the experimental response. The model of the interface element is designed as a line of 3D node- to -node contact elements with coincident nodes (Taufik *et al*., 2011), which connects the nodes at the back of the angles to the corresponding nodes at the column and beam flange and/or web. The normal stiffness value and sticking stiffness value are based upon the maximum expected force divided by the maximum allowable surface displacement. High contact stiffness was specified to prevent excessive penetration of the contact nodes.Shell elements were considered more appropriate for the beam, column and angle elements because they can provide a more efficient geometry modeling and analysis.

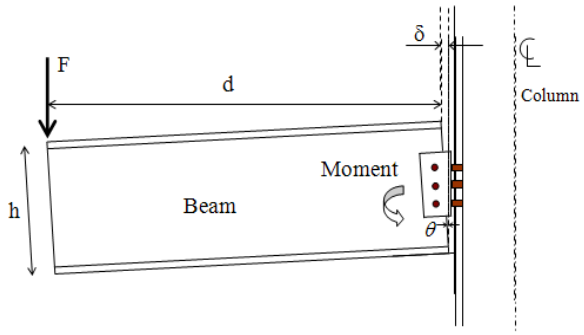

Fig. 4: Measurement of rotational angle change

The external monotonic static point load is applied in increments to obtain a converged solution in a nonlinear analysis. The automatic time stepping with a minimum time step increment is selected to obtain load sub- step result especially during the last step. The convergence criteria are based on the force and displacement for tracking the maximum plastic strain step. The deformation measurement is based on the deformation of the angle. The relative displacements at the locations of the beam tension and compression flanges were used to find the rotation of the connection. The rotation of the connection is defined as the relative horizontal displacement over the depth of the beam measured from the center of the top flange to the centre of the bottom flange.

The most important aspect of connection behavior is the moment-rotation (M-ϕ relationship. Stiffer connections will result in higher M-ϕ curves. The moment rotation curve of the connection is based on the following simple relations: M = Fd, ϕ = arctan (δ/h); where M is the moment, ϕ is the rotation of the connection, F is twice as much as the applied point load, d is the length of the beam, δ is relative displacement of the beam and h is the depth of the beam measured from the centre of the top flange to the centre of the bottom flange. Figure 4 shows the details of the rotational angle measurement when a load is applied.

Mild carbon steel S275was used for the beams and column with a yield stress of 300MPa and a Young modulus of 210 GPa. High strength bolt M20 grade 8.8 steel with a yield stress of 800 MPa is used for all types of the connections. The multi-linear elastic-plastic approach is used to determine the material properties of the beams, columns and angles for the FE model. The steel properties of S460, S550 and S690 have Young's modulus values of 205,000 MPa, 202,000 MPa and 200,000 MPa, respectively. Different material strengths have been used for the flat (f) regions($\sigma_{u,f}$) and the curve(c) regions ($\sigma_{u,c}$).The material properties of carbon steel grade S275 and high strength steel grades S460, S550 and S690 are used for the FE model with stress-strain curve as shown in Table 1; the Poisson's ratio is 0.3.

Table 1: Summary of the material properties

Grade	f_y(MPa)	f_u(MPa)	f_u/f_y	ε_u(%)	$\varepsilon_u/\varepsilon_y$
S460(b)$_{,f}$	480.0	580.0	1.208	20.00	41.67
S460(b)$_{,c}$	520.0	620.0	1.192	20.00	39.22
S550(c)$_{,f}$	570.0	650.0	1.140	16.00	38.30
S550(c)$_{,c}$	610.0	690.0	1.131	16.00	31.37
S690(d)$_{,f}$	875.0	915.0	1.046	14.00	21.54
S690(d)$_{,c}$	890.0	925.0	1.039	14.00	20.89

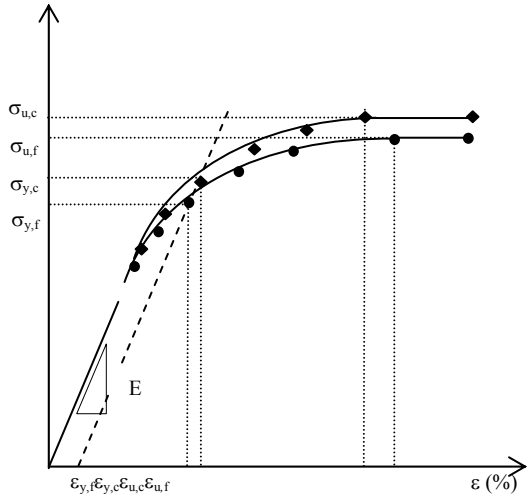

Fig. 5: Multilinear stress-strain curves for the FE model

The multilinear elastic-plastic approach is used to determine the material properties of the high strength steel for the FE model and the yield stress is defined as 0.2% proof stress, as shown in Fig. 5.

The angle cleats are modeled as radiused corner sections with enhanced strength regions. Strength enhancement due to cold-forming at the corners of the carbon steel sections was first studied by Karren (1967). Based on the examination of a substantial amount of test data, Karren (1967) proposed two analytical models to predict the changes caused by cold-forming at the corners. The r_i/t ratio was identified as having a significant effect on the corner strength; a decrease in ther_i/t ratio caused an increase in the corner strength. The σ_u/σ_y ratio of the virgin material was also identified as an important parameter. ENV 1993-1-3 (1996) accounts for the enhanced strength of the corners in the design of cold-formed carbon steel sections by allowing for an increase in the average strength of the entire section. The average yield strength f_{ya} is defined by Eq. (1). It should be noted that ENV 1993-1-3 (1996) only allows strength enhancements for cross-sections that are fully effective:

$$f_{ya} = f_{yb} + (f_u - f_{yb})\, knt^2/A_g \quad (1)$$

but, $f_{ya} \leq (f_u + f_{yb})/2$

where,

f_{yb} = The nominal yield strength

A_g = The gross cross-sectional area

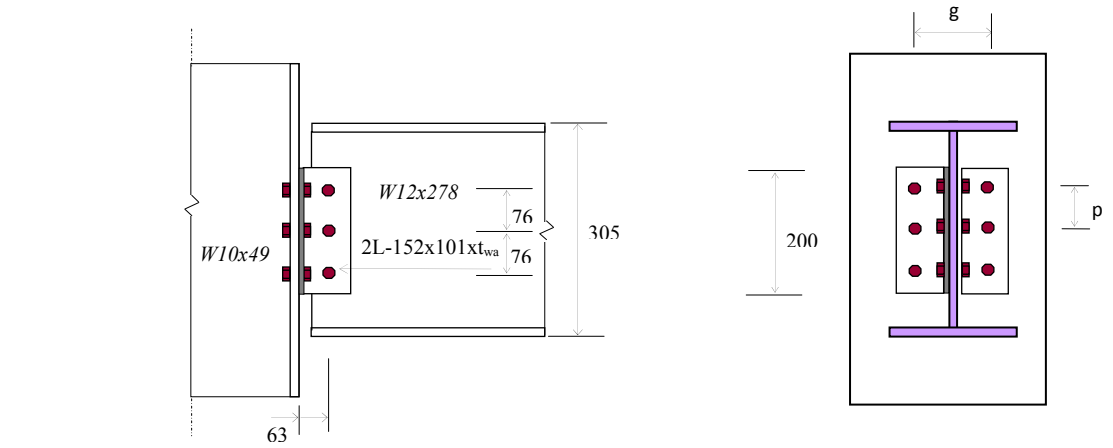

Fig. 6: The geometry of the DWA-1 connection (unit: mm)

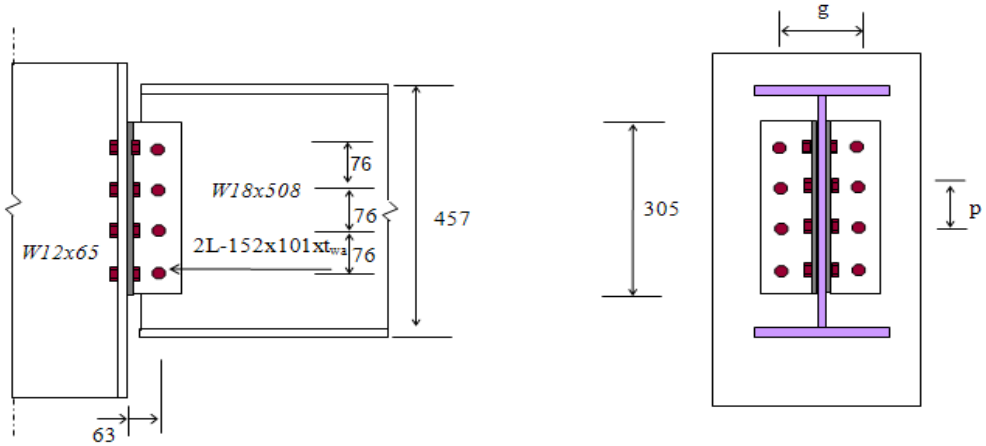

Fig. 7: The geometry of the DWA-2 connection (unit: mm)

k = 7 for cold-rolling
k = 5 for other methods of forming
n = The number of 90° bends in the cross-section with internal radii of $r \leq 5t$ (fractions of the 90° bends should be counted as fractions of n)
t = The nominal core thickness t_{cor} of the steel material before cold-forming, excluding zinc or organic coatings.

To establish the effects of angle configurations, the angle thickness and strength are selected as the two primary parameters. By combining these parameters, various moment-rotation curves can be obtained from 3D nonlinear finite element analysis. To increase the connection capacity, the higher strength angles are evaluated using different thicknesses. The gage length, bolt spacing and diameter are maintained at constant values.

Threetypes of cold-formedangles are investigated:

- L152×101×9.5
- L152×101×11.0
- L152×101×12.5

The only difference between these three cases is the thickness of the angles, which are 9.5 mm and11.0 mm for the DWA-1connection and 9.5 mm and 12.5 mm for the DWA-2 connection. For the DWA-1 connection aW12x27 beam and aW10x49 column are applied with an M19 bolt, whereas for the DWA-2 connection, a W18x50beam and a W12x65 column are applied. The connection geometry is shown in Fig. 6 and 7. The connection parameters are depicted in Table 2. The beam and column for DWA-1 and DWA-2 are design as different sizes. The bolt is made of M19 grade 8.8 and the gage on the column is 63 mm. The bolt hole is simplified by using a hexagonal shape model.

FINITE ELEMENT VALIDATION

The results of the FE analysis for the DWA connection are presented in comparison with the test results. Comparisons are made with the experimental results obtained from the literature (Lewit *et al*., 1996). The finite element models were validated against the recorded load-displacement curves from the tests.

Table 2: DWA connection parameters

Connection	Beam	Web angle (1)	Web angle (2)	g (mm)	p (mm)
DWA-1a	W12×27	L-152×101×9.5	L-152×101×9.5	63.0	76.0
DWA-1b	W12×27	L-152×101×11.0	L-152×101×11.0	63.0	76.0
DWA-2a	W18×50	L-152×101×9.5	L-152×101×9.5	63.0	76.0
DWA-2b	W18×50	L-152×101×12.5	L-152×101×12.5	63.0	76.0

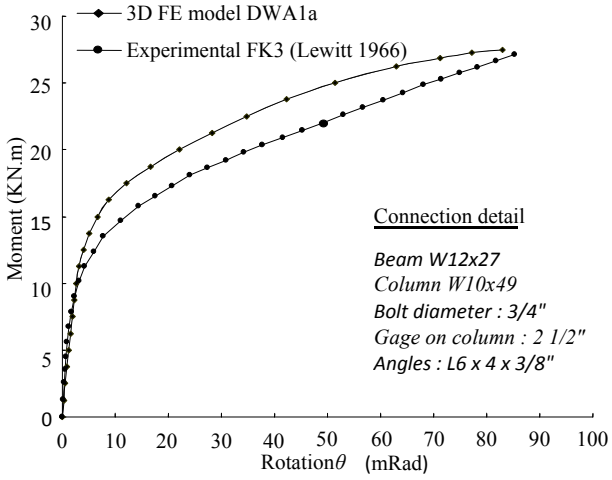

Fig. 8: A comparison of DWA-1a *M-θ* curves between the experimental and FE models

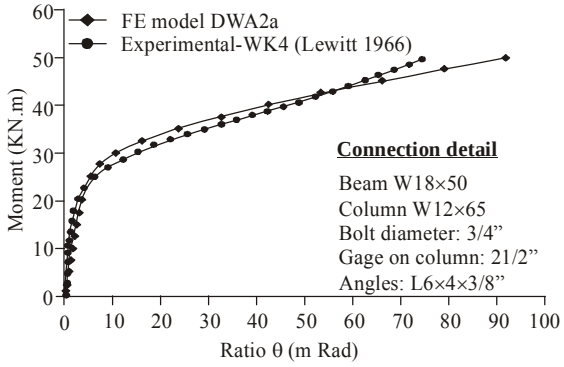

Fig. 9: A compariosonof DWA-2a *M-θ* curves between experimental and FE models

The analysis result for the DWA connections are presented in Fig. 8 and 9 for the three and four bolt rows configurations. The FE models show ultimate moments of 26.4 KN/m and 60.1KN/m, for the three and four bolt rows configurations respectively. The *M-θ* curve shape of the DWA connections determined from the experimental and theoretical results shows a difference due to a lack of data regarding the material properties from experimental testing. Bi-linear elastic perfectly plastic approach for the stress-strain curve is assumed in FE analysis.

To further investigate the difference between the response of the connection when a hexagonal hole is used and when a circular hole is used, the stress contours at the maximum capacity are shown in Fig. 10.The refined model with a circular hole and a shank with twelve spar elements gives a good prediction of the connection behavior. The maximum stress values are nearly the same at 456 MPa, because the hole area and the shank cross section area are kept equal.

Table 3: Strength enhancement parameters of the corner region

Connection	t_a(mm)	r_i/t_a	r_i(mm)	$r_i + 2t_a$ (mm)
DWA-1	9.5	0.74	7.0	26.0
DWA-2	11.0	0.55	6.0	28.0
DWA-3	11.0	0.55	6.0	28.0
DWA-4	12.5	0.40	5.0	30.0

EXTENTION OF STRENGTH REGIONS

Previous research has shown that enhanced strength is areas other than the curves corner should be included in numerical models to achieve the exact replication of the test results (Gardner and Nethercot, 2004). Karren (1967) found that for carbon steel sections, the effect of cold-forming extends beyond the corner to a distance approximately equal to the thickness (t), whereas Abdel-Rahman and Sivakumaran (1997) observed increased yield strengths up to a distance of $0.5\pi r_i$ beyond the corner. A parametric study was performed to investigate the extent to which corner enhancement extends beyond the curved region. Maintaining all other parameters at constants values, two different cases were studied, when the enhanced strength is localized in the curved corner region and, when the enhanced strength region is extended to a distance t_a beyond the corner, as shown Fig. 11. The various investigated parameters of strength enhancement are shown in Table 3.

Variable thicknesses of higher strength web angles (t_{wa}) are applied. The web angles are determined using different high strength steel grades, while the beam and column are consistently formed of with mild carbon steel. Table 4 indicates the observed failure moments from the finite element analyses. The ultimate moments from the FEanalysiswith corner strength enhancement extended to a distance t_a [M_{ult} FE (r_m+2t_a)] are compared to those determined with no corner strength enhancement [M_{ult} FE (ncs)]. The ultimate moment with corner strength enhancement in the region of r_m+2t_a is slightly increased compared with no corner strength enhancement. The difference between two approaches is only about 1%.

EFFECT OF WEB ANGLE THICKNESS

Various thicknesses of high strength cold-formed angles have been used in this study. The moment-

Table 4: Moment capacity and failure mode

Connection destination	Bolts in row	t_a (mm)	r_m (mm)	$M_{ult}FE_{(ncs)}$ (KN.m)	$M_{ult}FE(r_m+2t_{a)}$ (KN.m)	Failure mode
DWA1-b	3	9.5	7.0	25.3	25.6	Angle yielding
DWA1-c	3	9.5	7.0	27.4	28.1	Angle yielding
DWA1-d	3	9.5	7.0	32.3	32.8	Angle yielding
DWA2-b	4	11.0	6.0	59.0	60.0	Angle yielding
DWA2-c	4	11.0	6.0	64.6	64.8	Angle yielding
DWA2-d	4	11.0	6.0	74.4	75.0	Angle yielding
DWA3-b	3	11.0	6.0	34.5	35.0	Angle yielding
DWA3-c	3	11.0	6.0	36.9	38.1	Angle yielding
DWA3-d	3	11.0	6.0	42.0	42.4	Angle yielding
DWA4-b	4	12.5	5.0	73.7	75.0	Angle yielding
DWA4-c	4	12.5	5.0	79.1	80.0	Angle yielding
DWA4-d	4	12.5	5.0	92.2	93.0	Angle yielding

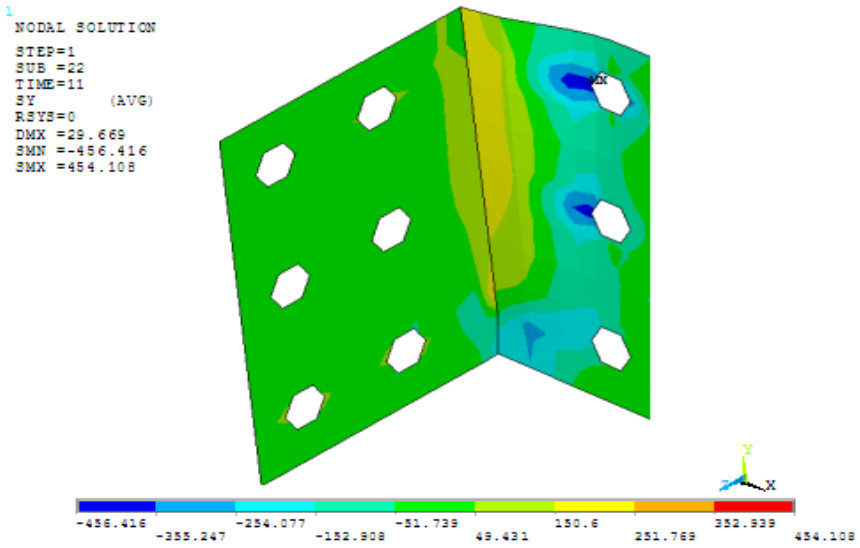

(a)

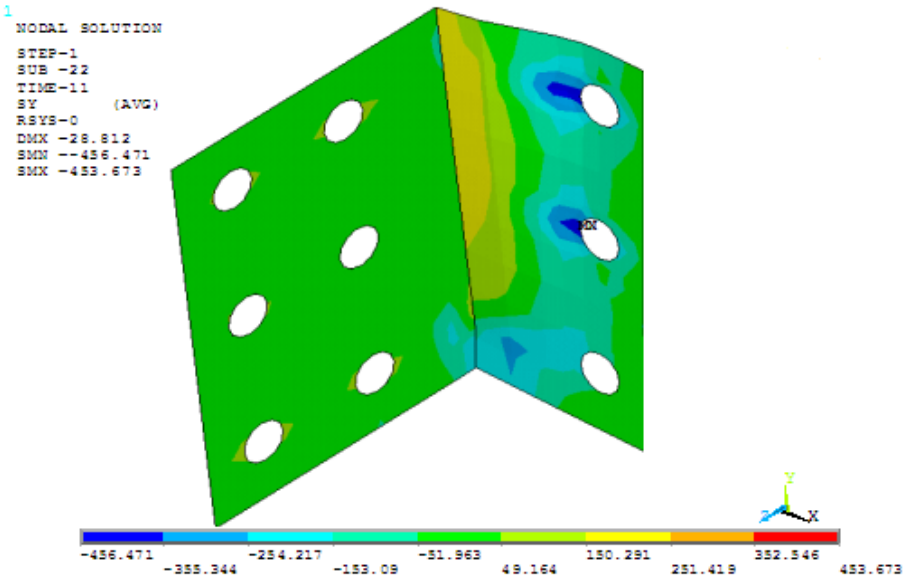

(b)

Fig. 10: Maximum stress of, (a) The web angles with hexagonal holes, (b) The web angleswith circular holes (in MPa)

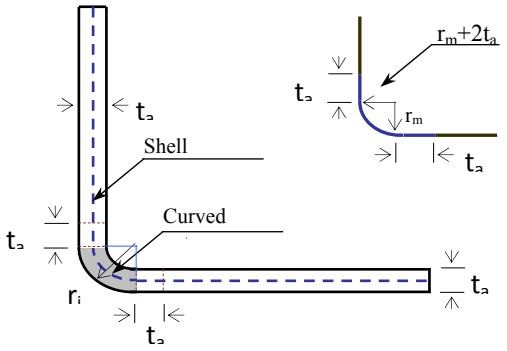

Fig. 11: Enhanced strength region of a cold formed angle

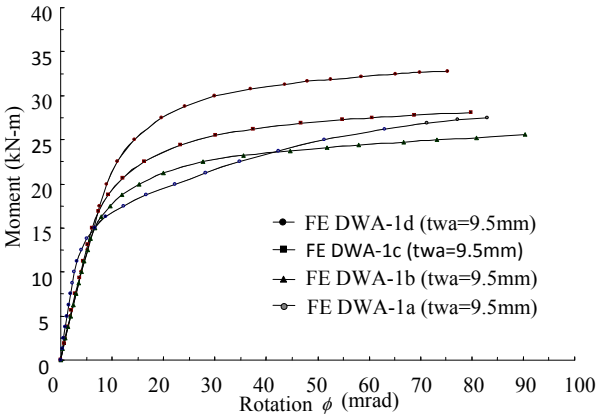

Fig. 12: Moment rotation curves ofthe DWA-1 configuration

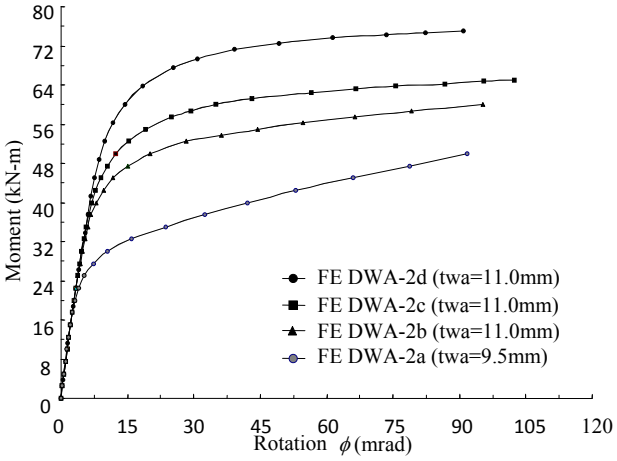

Fig. 13: Moment-rotation relationship of the DWA-2 model

rotation curves of the DWA connection from the FE model with corner strength enhancement are shown in Fig. 12 to 15.

The effect of the angle thickness and strength is more pronounced on the rotational capacity with the thinner angle. The initial stiffness is slightly higher with the thicker angle, while the rotational capacity is lower. The moment capacity of the S690 DWA is higher than moment capacity of the S460 DWA by up to 30% for

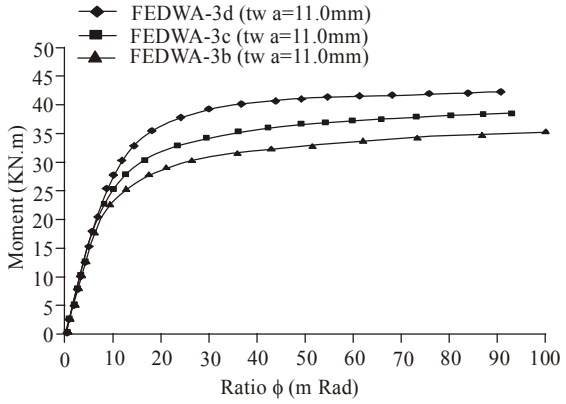

Fig. 14: Moment-rotation relationship of the DWA-3 model

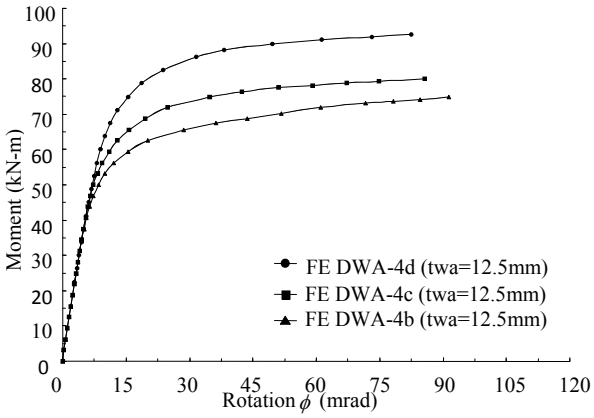

Fig. 15: Moment-rotation relationship of the DWA-4 model

the thinner angle (t_{wa}= 9.0 mm), but only up to 24% for the thicker angle (t_{wa}=12.5 mm) due to the excessive deformation around the larger curved corner region.

The moment capacity of the S550 DWA is higher than that of the S460DWA by up to 10% for thinner angle, but only up to 7% for the thicker angle. The moment capacity is still far below the ultimate moment of the maximum plastic strain limit, whereas the yield occurs earlier. As the initial stiffness of the connection is governed by the geometry of the web angle, the non-linear behavior is related to the material properties (strain hardening). The curve trend of DWA-1ain Fig. 12 is different from the curve trends of other models due to fact that the angles using hot rolled section with mild carbon steel and cold formed section with high strength steel.

The FE model of the DWAconnection with a thin angle and low beam depth shows significant results. The finite element model was used to confirm the predictions by studying the yielding of the angle and the column flange. Plots of the Von Mises equivalent plastic strain were used to assess the predicted yield line patterns due to angle yielding.

STRESS AND STRAIN PATTERN

To investigate the behavior of the connection, the stress contours of the angles are compared with those of the column flange. The patterns of the stress contours of the column flanges and angles with different grades and angles thickness are similar, with differences only observed in the value and the spread of the plasticity. The S550 web angles and S275 column flange stresses, as expected, are less than the ultimate stresses. Figure 16 illustrate that the maximum stresses of the angles are located at the corner region and beside the bolt hole.

ANALYTICAL MODEL FOR THE MOMENT-ROTATION RELATIONSHIP

The stiffness of any PR connection is dependent upon the moment-rotation characteristic associated with the connection. Many attempts have been made to establish curve-fitting techniques that can be used to provide suitable models for PR connections. Abolmaali *et al.* (2005) has developed moment–rotation model equations for flush end-plate connections. It was shown that both models predicted the M-θ plots closely, with the more accurate model being the three-parameter power model. The three-parameter power model was originally proposed by Richard and Abbott (1975) and Chen and Kishi (1989) to predict the moment-rotation (M-θ) characteristics of PR connections. Taufik *et al*. (2011) proposed a refined four-parameter power model to predict the moment-rotation curve of beam-column connection with high strength steel.

The *M-θ* data points obtained from these analyses were curve fitted to Equations 2 and 3 by least-square regression analysis to obtain model parameters M_u, *n, q and* θ_0. Consequently, regression equations were developed for the aforementioned parameters of each equation in terms of the geometric variables of the connection region. Three parameters are expanded into a proposed equation to accommodate changes in the curve shape due to the non-linear behaviors of the different steel grades used to construct each component of the connection. The rigidity parameter *n* will be substituted into parameter *q*, with the dependent variables considered. Thus, the prediction equation is defined as:

$$M = \frac{R_{ki}\theta}{\left[1+(\theta/\theta_0)^n\right]^{\frac{1}{q}}} \quad (2)$$

where,

M_u = Ultimate moment capacity
n = Rigidity parameter
q = Rigidity parameter
R_{ki} = Initial connection stiffness
θ_0 = Reference plastic rotation defined by:

$$\theta_0 = M_u / R_{ki} \quad (3)$$

In this study, several test cases were selected using the FE model of connection developed in the previous section. The *M-θ* data points obtained from the analysis were curve fitted to obtain model parameters. Consequently, regression equations were developed for the aforementioned parameters of each equation in terms of the geometric variables of the connection region. In the development of the prediction equations, the independent variables (geometry of the connection) are defined as:

g = The gage distance
d_b = The nominal bolt diameter
p_f = The bolt pitch
h_b = The beam depth
t_{wa} = The thickness of web angle
F_{ya} = Material yield stress of web angle
$E_{o,a}$ = Young's modulus of angle
$E_{o,c}$ = Young's modulus of corner

Unit of independent variables: mm and N/mm^2

Using these results and the multiple regression technique, a prediction equation was developed for each independent parameter using the following general form:

$$R_{ki} = \prod_{j=1}^{m} A a_j^{wj}; \qquad M_u = \prod_{j=1}^{m} B a_j^{xj}; \qquad n = \prod_{j=1}^{m} C a_j^{yj}; \qquad q = \prod_{j=1}^{m} D a_j^{zj} \quad (4)$$

where, A, B, C and D are unknown coefficients, a_j is the *j*th independent parameter, w_j, x_j, y_j and z_j are the exponents to be determined through regression and m is the number of independent parameters considered. By taking the logarithms of both sides of the formulas in Eq. (4), linear forms of these formulas are obtained as:

$$\ln R_{ki} = \ln A + \sum_{j=1}^{m} w_j \ln a_j \quad (5)$$

$$\ln M_u = \ln B + \sum_{j=1}^{m} x_j \ln a_j \quad (6)$$

$$\ln n = \ln C + \sum_{j=1}^{m} y_j \ln a_j \quad (7)$$

$$\ln q = \ln D + \sum_{j=1}^{m} z_j \ln a_j \quad (8)$$

Multiple regressions using spreadsheet software are applied to each formula in Eq. (5-8) to determine the coefficients A, B, C, D, w_j, x_j, *yj* and z_j. From these regression analyses, Eq. (9-12) represent the independent parameters of the design equation for the

Table 5: Parameter valuesfor the power model obtained through curve fitting

Connection destination	R_{ki} (kNm/mrad)	M_{uc} (kN.m)	Rigidity parameter (n)	Rigidity parameter (q)	Correlation coefficient (r)
DWA-1b	3.20	25.63	1.35	1.36	0.9995
DWA-1c	3.15	28.12	1.52	1.53	0.9994
DWA-1d	3.10	32.75	1.69	1.70	0.9992
DWA-2b	8.45	60.00	1.35	1.36	0.9993
DWA-2c	8.32	64.75	1.52	1.53	0.9992
DWA-2d	8.01	75.00	1.69	1.70	0.9991
DWA-3b	4.40	35.00	1.35	1.36	0.9992
DWA-3c	4.35	38.12	1.52	1.53	0.9991
DWA-3d	4.20	42.40	1.69	1.70	0.9992
DWA-4b	10.15	75.00	1.35	1.36	0.9941
DWA-4c	9.80	80.00	1.52	1.53	0.9885
DWA-4d	9.60	93.00	1.69	1.70	0.9990

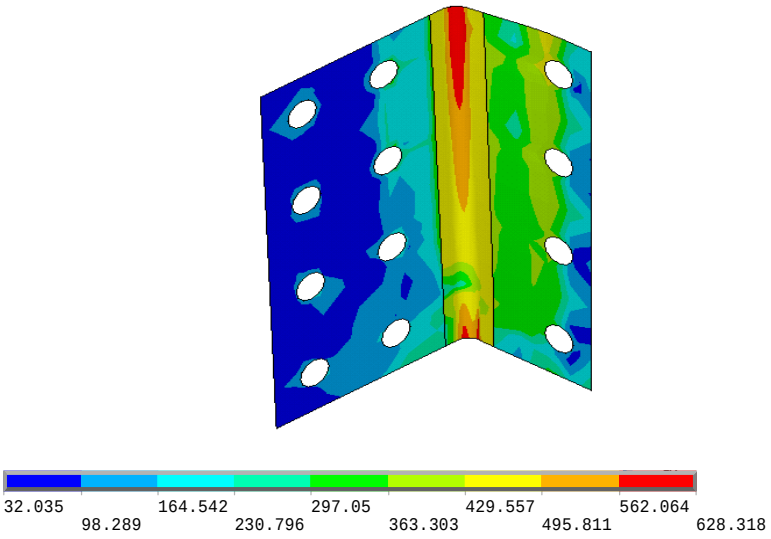

(a)

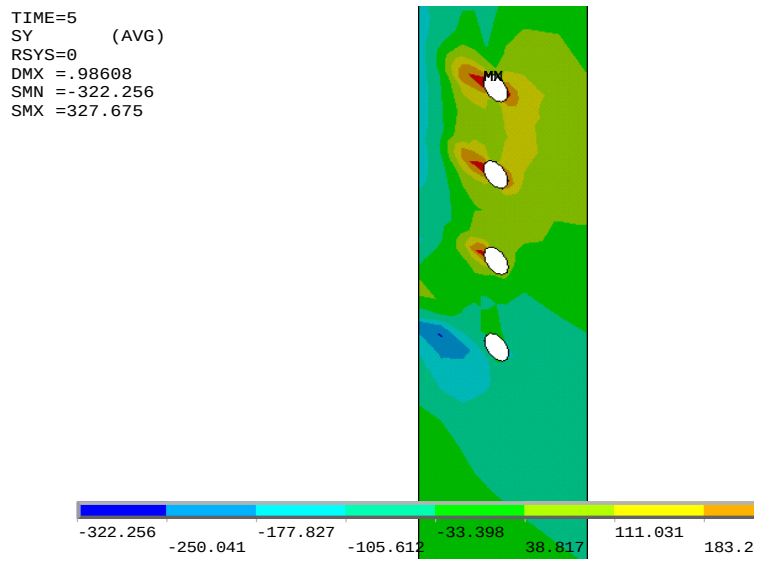

(b)

Fig. 16: Stress contours of, (a) The S550web angle, (b) The S275 column flange, (in Mpa)

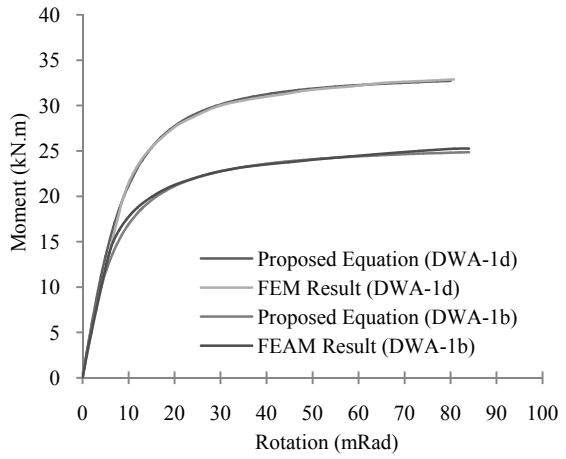

Fig. 17: Comparison of FEM results with proposed equation; DWA-1d and 1b models

ultimate moment, reference plastic rotation and rigidity parameter. Sensitivity and error band analyses were conducted to validate the behavior of each equation regarding the variation of independent variables and the error associated with each equation, respectively.

The design equations for the four dependent parameters of the double web angle connection are obtained as:

$$R_{ki} = 1.10 P_f^{0.77} h_b^{2.40} t_{wa}^{2.17} E_{0,a}^{1.25} E_{0,c}^{-1.25} \text{(N.mm/rad)} \quad (9)$$

$$M_u = 0.004\, d_b^{0.61} h_b^{2.10}\, t_{wa}^{2.13} F_{ya}^{2.17} \text{(N.mm)} \quad (10)$$

$$n = 0.02\, d_b^{-0.24} F_{ya}^{0.78} \quad (11)$$

$$q = 0.02\, d_b^{-0.23} F_{ya}^{0.78} F_{yc}^{0.01} \quad (12)$$

Table 5 presents the parameter values for the power model obtained through curve fitting of the data regarding the high strength DWA connection.

Comparisons of the m-θ results (Fig. 17) for model the DWA-1d model (S690 web angle) and the DWA-1b model (S460 web angle) generated by the proposed equation are compared with those obtained from FE model. The curves in the figure clearly show that the two curves are in good agreement for each curve.

CONCLUSION

A three-dimensional finite element model of a bolted connection is presented. The properties of four different steel grades used to construct web angles are investigated. The following conclusions are drawn based on the research:

- The initial stiffness of the FE model is well predicted, as determined by verification with previous experimental results. A less pronounced effect of higher yield stress on the initial stiffness of the connection is demonstrated. Angles that are thicker and higher in strength are associates with larger values of initial stiffness and moment capacity.
- The plastic strain and stress patterns of high strength web angle are generally very similar, as are those of high strength top and seat angles. The model presented gives excellent results for significantly increasing the moment and rotational capacity.
- The high strength angles contribute a significant proportion of the maximum stress distribution, when the beam and column are formed of mild carbon steel. Taking into account the strength enhancement of the corner regions allows for a slight increase in the ultimate moment capacity.
- A four-parameter power model expression was proposed to predict the ultimate moment and initial stiffness of the high strength DWA connection. The expression is a function of the corresponding strength of the web angles. A reasonable prediction was obtained for the behavior of the high strength PR connection.

REFERENCES

Abdel-Rahman, N. and K.S. Sivakumaran, 1997. Material properties models for analysis of cold-formed steel members. J. Struct. Eng. ASCE, 123(9): 1135-1143.

Abolmaali, A., J.H. Matthysa, M. Farooqib and Y. Choic, 2005. Development of moment-rotation model equations for flush end-plate connections. J. Construct. Steel Res., 61: 1595-1612.

Bahaari, M.R. and A.N. Sherbourne, 1996. 3D simulation of bolted connections to unstiffened columns-II extended endplate connections. J. Construct. Steel Res., 40(3): 189-223.

Bose, B., S. Sarkar and M. Bahrami, 1996. Extended endplate connections: Comparison between three-dimensional nonlinear finite-element analysis and full-scale destructive tests. Struct. Eng. Rev., 8(4): 315-328.

Bursi, O.S. and J.P. Jaspart, 1998. Basic issues in the finite element simulation of extended end plate connections. Comp. Struct., 69: 361-382.

Chen, W.F. and N. Kishi, 1989. Moment-rotation relation of top and seat angle connections. Proceedings of the International Colloquium on Bolted and Special Connections, CE-STR-87-4.

Citipitouglu, A.M., R.M. Haj-Ali and D.W. White, 2002. Refined 3D finite element modeling of partially restrained connections including slip. J. Construct. Steel Res., 58(5-8): 995-1013.

Danesh, F., A. Pirmoz and D.S. Daryan, 2007. Effect of shear force on the initial stiffness of top and seat angle connections with double web angles. J. Construct. Steel Res., 63(6): 1208-1218.

ENV 1993-1-3, 1996. Design of steel structures, Part 1-3, General rules, supplementary rules for cold formed thin gauge members and sheetings. European Committee for Standardisation.

Gardner, L. and D.A. Nethercot, 2004. Numerical modelling of stainless steel structural components-a consistent approach. J. Struct. Eng. ASCE, 130(10): 1586-1601.

Guoa, Y.J., A.Z. Zhu, Y.L. Pi and F. Tin-Loi, 2007. Experimental study on compressive strengths of thick-walled cold-formed sections. J. Construct. Steel Res., 63: 718-723.

Karren, K.W., 1967. Corner properties of cold-formed steel shapes. J. Struct. Divis. ASCE, 93(ST1): 401-432.

Lewitt, C.W., E. Chesson Jr and W.H. Munse, 1996. Restraint Characteristics of Flexible Riveted and Bolted Beam-to-Column Connections. Structural Research Series, University of Illinois, Urbana-Champaign, No. 296.

Maggi, Y.I., R.M. Goncalves, R.T. Leon and L.F.L. Ribeiro, 2005. Parametric analysis of steel bolted end plate connections using finite element modelling. J. Construct. Steel Res., 61(5): 689-708.

Moze, P. and D. Beg, 2011. Investigations of high strength steel connections with several bolts in double shear. J. Construct. Steel Res., 67(3): 333-347.

Puthli, R. and O. Fleischer, 2001. Investigations on bolted connections for high strength steel members. J. Construct. Steel Res., 57(1): 313-326.

Richard, R.M. and B.J. Abbott, 1975. Versatile elastic-plastic stress-strain formula. J. Eng. Mech. Divis. ASCE, 101(4): 511-515.

Sherbourne, A.N. and M.R. Bahaari, 1996. 3D simulation of bolted connections to unstiffened columns-I. T-stub connections. J. Construct. Steel Res., 40(3): 169-187.

Taufik, S. and R.Y. Xiao, 2005. 3D finite element predictions of angle bolted connection with high strength steel. Proceeding of the 4th International Conference on Advance in Steel Structures, Shanghai-China, 2: 1775-1782.

Taufik, S. and R.Y. Xiao, 2006a. Simplified finite element modelling of beam-column bolted connection with shell element. Proceeding of the 8th International Conference on Computational Structures Technology, Las Palmas de Gran Canaria - Spain.

Taufik, S. and R.Y. Xiao, 2006b. Three-dimensional finite element modelling of flush end plate connection with high strength steel. Proceeding of the 8th International Conference on Computational Structures Technology, Las Palmas de Gran Canaria, Spain.

Taufik, S., S. Baharom and R.Y. Xiao, 2011. Predicted behaviour of partially restrained connection with cold formed high strength steel by 3D finite element modelling. Adv. Mater. Res., 250-253: 1734-1743.